BIOCHEMISTRY
including biophysical chemistry & molecular biology

Article

pubs.acs.org/biochemistry

Interaction of Doxorubicin with Polynucleotides. A Spectroscopic Study

Marta Airoldi,[†] Giampaolo Barone,[†] Giuseppe Gennaro,[†] Anna Maria Giuliani,[†] and Mauro Giustini*[,‡]

[†]Dipartimento STEBICEF, Università di Palermo, Viale delle Scienze, Parco D'Orleans, Pad. 17, 90128 Palermo, Italy

[‡]Dipartimento di Chimica, Università "La Sapienza", P. le Aldo Moro 5, 00185 Roma, Italy

Supporting Information

ABSTRACT: The interaction of doxorubicin (DX) with model polynucleotides poly(dG-dC)·poly(dG-dC) (polyGC), poly(dA-dT)·poly(dA-dT) (polyAT), and calf thymus DNA has been studied by several spectroscopic techniques in phosphate buffer aqueous solutions. UV−vis, circular dichroism, and fluorescence spectroscopic data confirm that intercalation is the prevailing mode of interaction, and also reveal that the interaction with AT-rich regions leads to the transfer of excitation energy to DX not previously documented in the literature. Moreover, the DX affinity for AT sites has been found to be on the same order of magnitude as that reported for GC sites.

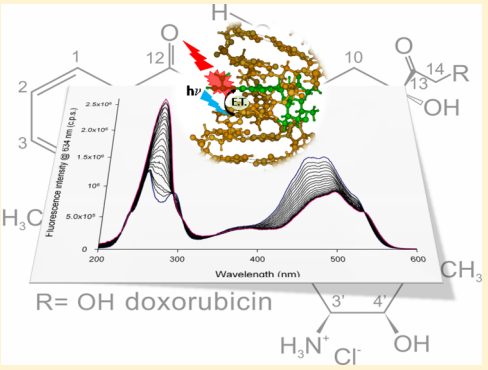

The anthracyclines[1] make up a class of antibiotics originally derived from a soil bacterium, *Streptomyces peucetius*. They are among the first chemotherapeutic agents developed and the most widely used, active against a large variety of tumors (leukemia, lymphoma, cancer of the breast, lung, ovaries, etc.). The first anthracyclines were isolated early in the 1960s and were named doxorubicin (DX) and daunorubicin (DNR). As shown in Chart 1, DX and DNR share aglyconic and sugar moieties. The aglycone consists of a tetracyclic ring system with adjacent quinone-hydroquinone groups in rings C and B, a methoxy substituent at C-4 in ring D, and a short side chain at C-9 in ring A with a carbonyl at C-13. The sugar, called daunosamine, is attached by a glycosidic bond to C-7 of ring A. The only difference between DX and DNR is that the side chain of DX terminates with a primary alcohol whereas that of DNR terminates with a methyl.

Chart 1. Chemical Formula of Anthracyclines

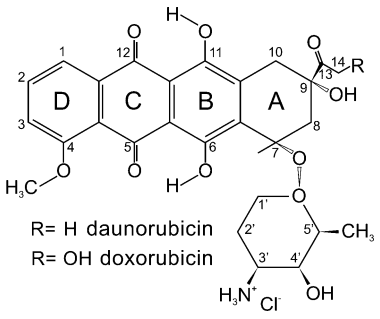

The genetic material in living cells consists of deoxyribonucleic acid (DNA). At its lowest organization level, the three-dimensional structure of DNA is rather simple. Hydrogen-bonded base pairs are stacked like coins in a roll along the axis of a right-handed double helix with the sugar−phosphate backbones of each strand on the outside, winding up in an antiparallel orientation. The interstrand hydrogen bonding patterns impose limitations on the ability of the base pairs to be used as molecular recognition targets, so the features that first are recognized by low-molecular weight ligands are found along the major and minor grooves that lie between the phosphodiester linkages in both strands.[2]

There are indeed several ways by which molecules ("ligands") can interact with DNA. Ligands may interact with DNA by covalent and noncovalent binding, including intercalation. Intercalation is a process in which small molecules with a planar aromatic or heteroaromatic ring system of appropriate dimensions and geometry fit themselves between adjacent base pairs of DNA. As a consequence, intercalation involves an increase in the vertical separation between adjacent base pairs and partial unwinding of the double helix, causing changes of the twist angle and distortions of the sugar−phosphate backbone.[3,4]

Despite their long history as anticancer agents, there is still considerable mystery about the mechanism of action of the anthracyclines. Nevertheless, the biological activity of these molecules is likely associated with their DNA binding properties, and there is evidence that antitumor activity is essentially due to the intercalation in the base pairs of DNA.[5] Intercalation of the anthracyclines into the double helix of DNA

Received: December 20, 2013
Revised: March 18, 2014
Published: March 18, 2014

   dx.doi.org/10.1021/bi401687v | *Biochemistry* 2014, 53, 2197−2207

can be easily monitored by fluorescence spectroscopy because anthracyclines are excellent fluorophores, but intercalation causes a strong fluorescence quenching.[6−10] Thus, it is possible, at least in principle, to obtain an anthracycline−polynucleotide binding constant for the intercalation process by measuring fluorescence quenching. Other types of interactions such as, for instance, groove binding can be evidenced by other techniques, like UV−vis absorption spectroscopy and circular dichroism (CD).[11−13]

We report here the study of the interaction of doxorubicin with the synthetic polynucleotides poly(dG-dC)·poly(dG-dC) (polyGC) and poly(dA-dT)·poly(dA-dT) (polyAT) as well as calf thymus DNA (ct-DNA). Despite the conspicuous number of publications on this topic, the details of the interactions of DX with the genetic material are still rather unclear. They are mainly based on the reported preferential interaction of DX with GC base pairs,[5,9,14,15] with little or no affinity for AT-rich regions.[14] With the aim of shedding some light on this issue, the interactions of DX with synthetic and natural polynucleotides have been studied via several noninvasive spectroscopic techniques (CD, UV−vis, steady state, and time-resolved fluorescence) as well as by molecular mechanics (MM) simulations.[16] As we will show, DX was revealed to have almost undistinguishable affinity for GC or AT regions, though the interactions in the two cases are somewhat different.

MATERIALS AND METHODS

Chemicals. The 1 mM phosphate buffer (PB) solution used in all the experiments was prepared by dissolving in twice distilled water the appropriate amount of $Na_2HPO_4{\cdot}12H_2O$ and adjusting the pH to the desired value (7.3 ± 0.2) by addition of controlled volumes of a 6.0 M hydrochloric acid solution. All chemicals were from Carlo Erba Reagents and were reagent grade.

PolyGC [sodium salt; MW = (5.3 ± 0.5) × 10^5 Da] and polyAT [sodium salt; MW = (1.4 ± 0.5) × 10^6 Da] were purchased from Sigma (Sigma-Aldrich Co.) in vials of 25 and 50 units, respectively (1 unit is defined as the amount of polymer that yields an absorbance of 1.0 at 260 nm when it is dissolved in 1.0 mL of water in a 1.0 cm optical path cuvette). Lyophilized samples of the two polynucleotides were prepared in Eppendorf vials as described elsewhere from the commercial vials[17] and stored over silica gel below 273 K.

ct-DNA (42% in GC base pairs) was obtained from Serva in vials of 250 mg and was used as received; stock concentrated solutions have been prepared by weighing the appropriate amount of the polymer in 1 mM PB buffer.

DX (MW = 580.0 Da) was a kind gift of Carlo Erba Reagents and its purity checked by ^{1}H nuclear magnetic resonance.

Lyophilized samples of DX were prepared in Eppendorf vials by aliquoting 200 μL of a stock solution of a known concentration (0.547 mg of DX, Mettler Toledo AT21 Comparator, dissolved in a 10 mL measuring flask with Milli-Q water) and following the same procedure described for polyGC and polyAT. Also in this case, the Eppendorf vials were stored over silica gel below 273 K. The concentration of each sample was then calculated from the absorbance at 480 nm using an ε value of 11500 M^{-1} cm^{-1}.[18] The appropriate dilution with 1 mM PB allowed the determination of the calibration plot from fluorescence data (see below), covering the concentration range between 4.19 × 10^{-8} and 3.13 × 10^{-6} M.

Instrumentation. Electronic absorption spectra were recorded and processed with a Cary 1E or Cary 50 Varian spectrometer, while CD spectra were acquired with a Jasco J715 spectropolarimeter equipped with a xenon lamp (150 W) under a nitrogen flux. The Cary 1E spectrometer, equipped with a Peltier temperature controller, was employed also for the determination of melting temperatures (T_m). The maximal wavelength range for spectral measurements was 210−600 nm. The temperature was controlled (±1 K) by means of either a Haake F3K or a Julabo FD thermostat.

Fluorescence spectra were recorded with a Fluoromax-2 Jobin Yvon-Spex spectrofluorimeter. Emission spectra were acquired in the wavelength range of 500−800 nm (the excitation wavelength, excitation and emission slits, filters in cases in which they were used, varied among different experiments, and the relevant information will be specified in due time). For the fluorescence excitation spectra, the fluorescence intensity at 634 nm has been recorded by varying the excitation wavelength in the range of 200−600 nm and by protecting the photomultiplier (PMT) by means of two Baird-Atomic red filters (BA 590 + BA 600), with both excitation and emission slits set at 5 nm. From the fluorescence emission spectra acquired in the range of 500−800 nm, via excitation of the samples at 410 nm with both excitation and emission slits set at 5 nm, of a series of DX solutions in 1 mM PB, a calibration plot was determined by calculating the area of each spectrum and by plotting it against the analytical DX concentration ($[DX]_a$): a straight line was obtained (Figure S1 of the Supporting Information). Assays at different NaCl concentrations, up to 0.5 M, gave essentially the same results, thus ensuring that self-aggregation of the drug does not take place in the range of DX and NaCl concentrations explored. Therefore, the same calibration plot was used throughout this work to obtain the concentration of free DX ($[DX]_f$) from the fluorescence emission spectra. The excitation wavelength of 410 nm was chosen because it allowed us to record the whole DX emission spectrum (500−800 nm) without any perturbation due to the water Raman band ($\lambda_{Raman@410}$ = 476 nm) whose interference can be only partially corrected by recording the baseline and that can severely bias the analytical reliability of $[DX]_f$ at the lowest DX concentrations.

The fluorescence lifetime measurements have been performed with home-built time-correlated single-photon counting (TCSPC) instrumentation. To take into account the PMT color effects, the instrument response function (IRF) has been measured at each detected wavelength by recording the time profile of the monoexponential fast decaying molecule Rose Bengal.[19] Details on the TCSPC instrumentation are given in the Supporting Information.

Hellma quartz suprasil cuvettes of the appropriate optical path length (either 1.0 or 5.0 cm) were used for the experiments.

A Radiometer PHM22 pH-meter equipped with a combined Hamilton microelectrode (pH 0−14) was employed for pH measurements.

Preparation of the Samples. Two types of titration experiments were performed, preparing a sample with a known concentration of doxorubicin or, alternatively, the polynucleotide and adding successive aliquots of a concentrated solution of the polynucleotide or doxorubicin. The change in volume never exceeded 10%. Samples and titrating solutions were prepared by dissolving the lyophilized content of an Eppendorf vial (previously described) in the appropriate volume of PB or PB/NaCl solutions.

The actual concentrations of the polynucleotides in monomer units, [PN-P], were obtained from the electronic spectra making use of the following parameters: ε_{254} = 8400 M^{-1} cm^{-1} for polyGC,[20] ε_{262} = 6650 M^{-1} cm^{-1} for polyAT,[21] and ε_{260} = 6600 M^{-1} cm^{-1} for ct-DNA.[22] All absorbance values were corrected for the background absorbance at a wavelength value at which the polymer or the drug does not absorb.

The samples are characterized by the value of R, defined as

$$R = \frac{n_{\text{PN-P}}}{n_{\text{DX}}}$$

where $n_{\text{PN-P}}$ and n_{DX} are the moles of polynucleotides (in monomer units) and DX, respectively.

The samples of doxorubicin for the fluorometric titration experiments with the three polynucleotides were prepared with a $[\text{DX}]_a$ value of $\leq$5 μM. This concentration threshold was chosen on the basis of preliminary fluorescence experiments, showing a linear correlation between the area of the fluorescence band and the concentration only up to that limit (see above). At higher concentrations, autoassociation of the drug caused a partial fluorescence quenching, leading to negative deviations from linearity (data not shown). In general, the doxorubicin concentration in all experiments was kept as low as possible ($[\text{DX}]_a \leq 5 \times 10^{-5}$ M), compatibly with the limitations imposed by the sensitivity of the method and by the time stability of the drug in solution, that did not allow overly long times for the completion of the experiment.[23−26]

Computational Details. Two alternating deoxydecanucleotide duplexes in the B-DNA conformation, d(ATATATATAT)$_2$ and d(GCGCGCGCGC)$_2$, have been built by the NUCLEIC routine of the TINKER software package,[27−29] using the Amber 99 force field[30] as recently reported.[31] The doxorubicin drug was inserted between the fifth and sixth stacked base pairs by opportunely modifying torsion angles α−ζ and χ of the sugar phosphate backbone in the intercalation pocket.[2] The geometry of the two drug−decanucleotide complexes was fully optimized by the Amber[32] method implemented in the Gaussian 03 software package.[33] The choice of the approximate computational method was imposed by the large size of the polynucleotide models considered, i.e., 628 and 638 atoms for d(GCGCGCGCGC)$_2$ and d(ATATATATAT)$_2$, respectively. In fact, it is known that accurate quantum chemistry calculations can be performed only on small oligonucleotide models.[34]

EXPERIMENTAL RESULTS AND DISCUSSION

This section has been organized in subsections, each referring to a particular experimental technique or a particular type of calculation. Dilution effects (when pertinent) were always considered when drawing the figures or making the calculations.

To describe the interaction of doxorubicin with the polynucleotides, we considered the following simple reaction scheme:

$$\text{binding site} + \text{doxorubicin} \rightleftarrows \text{bound doxorubicin}$$

Circular Dichroism and Absorption Studies. CD spectra of polyGC in the presence of increasing amounts of DX were recorded at 298 K in 1 mM PB in the absence of NaCl. The initial concentration of polyGC in monomer units was on the order of 1.8 × 10^{-5} M, and successive aliquots of a (4.5 ± 0.1) × 10^{-5} M solution of DX were added to explore the R range from 160 to 3.7, in several different series of experiments. Some relevant selected CD spectra of one of the series are shown in Figure 1. Upon addition of DX to polyGC, an ICD (induced

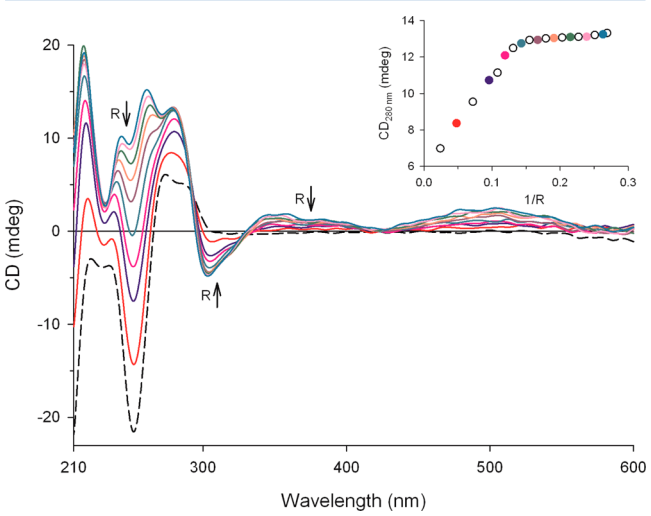

Figure 1. Titration of polyGC with doxorubicin: CD spectra (298 K, 1 mM PB buffer, pH 7.2; R from 42 to 3.7; initial $[\text{GC-P}]_a$ = 18.5 μM; the dashed line is the spectrum of polyGC alone; l = 5 cm). Empty symbols in the inset were taken from spectra not reported here for the sake of clarity.

circular dichroism) minimum appeared at ∼307 nm and a maximum grew at nearly 221 nm, which were blue-shifted and increased in amplitude as R was decreased from 160 to ∼5.6. At lower R values, the two bands, characteristic of the doxorubicin−polyGC complex, remained practically unchanged like that at 280 nm (see the inset in Figure 1), indicating the saturation of binding. Two isodichroic points were present for R values of >5.6 at 293 and 332 nm, suggesting a well-defined two-state equilibrium.

The characteristic CD maxima of doxorubicin in the visible spectral region increased with a decrease in R and were markedly red-shifted (from ∼470 to ∼504 nm); the amplitude of the bands was larger than expected on the basis of the analytical drug concentration (Figure S2 of the Supporting Information), indicating increased chirality due to rigid binding to the chiral duplex. The weak CD minima of doxorubicin in the 500−550 nm spectral region were undetectable. These CD features, together with the results of absorption studies (*vide infra*), are consistent with the formation of a strong, very likely intercalative, complex between DX and polyGC.[35−38] In the UV−vis spectra for the same samples with R values above ∼9, the band in the visible region (400−550 nm), due to DX alone, can reasonably be attributed to the drug bound to polyGC; thus, the absorbance at 480 nm was plotted against the analytical DX concentration, and a straight line was obtained. We concluded that only one species, i.e., bound DX, was present in the R range considered obeying the Beer−Lambert law. From the slope of the line ε_b, the molar absorption coefficient of bound DX was derived [ε_b = (5600 ± 400) M^{-1} cm^{-1} at 480 nm], consistent with the ε_b value reported for DNR-intercalating polyGC [ε_b = (7040 ± 250) M^{-1} cm^{-1}].[9] This result again suggests intercalation, leading to an increased number of π−π stacking interactions and thus lower ε values, as the prevailing mechanism for interaction between DX and polyGC.[35]

dx.doi.org/10.1021/bi401687v | *Biochemistry* 2014, 53, 2197−2207

In the same PB solution, in the absence of NaCl, titration of DX with polyGC was also performed with *R* values in the range of 0.0−2.0; a typical set of CD spectra is shown in Figure 2 with

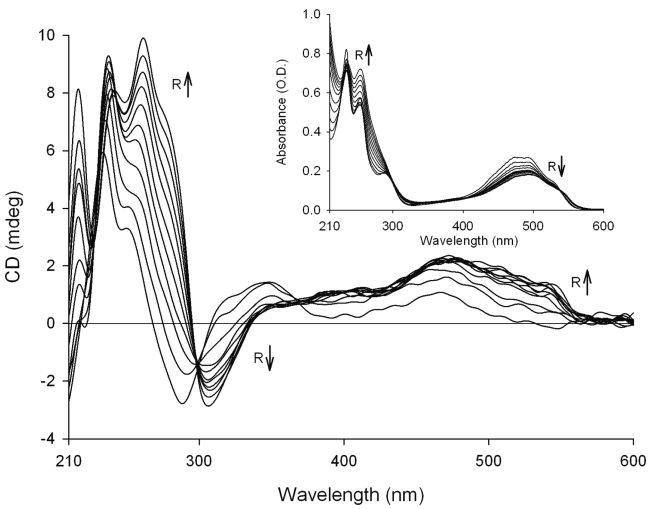

Figure 2. Titration of doxorubicin with polyGC: CD spectra (298 K; 1 mM PB, pH 7.2; initial $[DX]_a$ = 23.0 μM; *R* from 0.0 to 2.0; *l* = 1 cm). The corresponding UV−vis spectra are shown in the inset.

the corresponding UV−vis spectra in the inset. The characteristic feature around 300 nm, namely the free DX minimum at 289 nm that decreased with an increase in R while, in parallel, a new minimum attributed to bound DX grew at 304 nm with the appearance of an isodichroic point at 297.4 ± 0.4 nm, indicated the existence of a two-state equilibrium between free and bound drug. A second isodichroic point, not so well-defined, at ∼376 nm and the isosbestic point in the electronic absorption spectra at 538 nm point to the same conclusion. These features were lost at *R* values higher than ∼0.8.

The CD spectral behavior with an increase in the *R* value (*inter alia* red-shift and marked increase in the amplitude of the DX band in the visible region) and the clear hypochromicity of the drug absorbance in the same spectral region in the presence of the isosbestic point (inset in Figure 2) all point to the formation of a strong complex with DX rigidly bound in a highly chiral environment with enhanced $\pi-\pi$ stacking interactions. It is worth mentioning that in the interaction between DX and polyGC electrostatics also plays a crucial role. This is clearly evidenced by the reduced increase in the magnitude of the CD band in the visible region in the presence of increasing amounts of NaCl (Figure S3 of the Supporting Information). This point will be further evidenced and discussed in Binding Constant Determination.

For comparison, similar CD and absorption studies were performed on the DX−polyAT system. With the aim of exploring a large *R* range, either DX was titrated with polyAT (*R* = 0.0−1.3) or polyAT with DX (*R* = 0.6−6.0), taking care to have an overlapping *R* interval.

The CD spectra of a titration of the drug with polyAT are reported in Figure 3 with the corresponding UV−vis spectra shown in the inset. The CD minimum of the drug at 290 nm decreased during the course of the titration, while another minimum that could be attributed to the DX−polyAT complex developed around 308 nm. The presence of two isodichroic points at 297 ± 1 and 374 ± 2 nm, and of several isosbestic points, suggests the equilibrium between two species, which

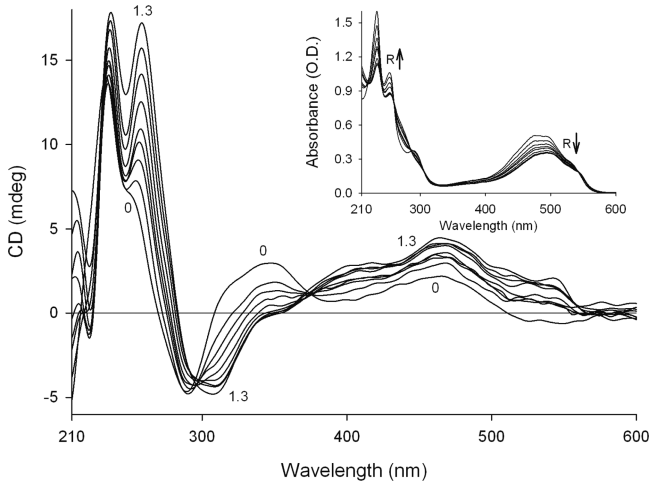

Figure 3. Titration of doxorubicin with polyAT: CD spectra (298 K; 1 mM PB, pH 7.3; initial $[DX]_a$ = 43.5 μM; *R* from 0.0 to 1.3; *l* = 1 cm). The corresponding UV−vis spectra are shown in the inset.

one can reasonably propose to be free DX and the DX−polyAT complex. The titration of polyAT with DX, instead, gave rise to CD spectra in which no isodichroic point was present, while the amplitude of the band centered at ∼500 nm increased with the addition of the drug and exhibited a marked blue shift, as observed also with polyGC (see above). A minimum developed at ∼300 nm, increasing in amplitude and shifting to a lower wavelength as *R* decreases; in the presence of an excess of doxorubicin ($R \leq 0.6$), it was found at the spectral position of the free anthracycline. The first addition of doxorubicin (*R* = 5.8) already caused the disappearance of the polyAT CD minimum at ∼250 nm, as well as a marked decrease in the absorbance at 260 nm in the UV−vis spectrum, and both features suggest the formation of a stable DX−polyAT complex. The last point is neatly evidenced in Figure S3 of the Supporting Information: such conspicuous hypochromicity suggests the formation of an intercalation complex, because intercalation promotes base stacking[39] and thus a decrease in absorbance.

For the polyGC−DX and polyAT−DX systems, the maximal ICD magnitude at 307 nm is less than 10 M^{-1} cm^{-1} (in $\Delta\varepsilon$ units), as expected for intercalation.[35,36,40]

Titration of DX with ct-DNA, for the sake of comparison, showed hypochromism and a red-shift of the absorption bands in the range of 400−600 nm, an increase in amplitude, and a red-shift of the CD bands in the same spectral region and the appearance of the low-intensity ICD minimum at 300 nm characteristic of bound DX. All these experimental findings clearly indicate intercalation as the mechanism of interaction, which has been well documented in the literature.[15]

PolyAT Melting Experiments. Intercalation of small molecules into the double helix is expected to increase the melting temperature (T_m) of the helix;[35,39,41−44] thus, some melting experiments were conducted for the polyAT−DX system to support the proposed intercalation mechanism of interaction. The corresponding studies could not be performed for the polyGC−DX system, because of the excessively high melting temperature of polyGC.[2] In detail, variable-temperature measurements were conducted for the DX−polyAT system in the absence of NaCl and in the presence of 25 mM salt, at *R* values of 2.0 and 1.0. For comparison, the melting temperature of polyAT at 25.0 mM NaCl was also re-evaluated, while in the

dx.doi.org/10.1021/bi401687v | *Biochemistry* 2014, 53, 2197−2207

absence of NaCl, polyAT is essentially already melted at 298 K.[17] The results are listed in Table 1. The very high ΔT_m values

Table 1. Melting Temperatures of the PolyAT−Doxorubicin System in 1 mM PB (pH 7.4)

[NaCl] (mM)	1/R = [DX]/[AT-P]	T_m (K)
0.0	1.0	358.1
0.0	0.5	357.0
0.0	0.0	<298
25.0	1.0	357.0
25.0	0.5	354.8
25.0	0.0	324.2

found strictly resemble those reported for the intercalation of the closely related DNR molecule into the polyAT double helix,[6] thus lending strong support to the intercalation of DX into the polyAT duplex.

Molecular Mechanics Calculations. To elucidate possible differences between polyAT and polyGC in their ability to intercalate doxorubicin, molecular mechanics calculations of the interaction were performed using decamer models of the two double helices. Drug intercalation occurs between residues 5 and 6 of the considered oligomers, and the intercalation models were obtained by the Amber method. In Figures 4 and 5, the

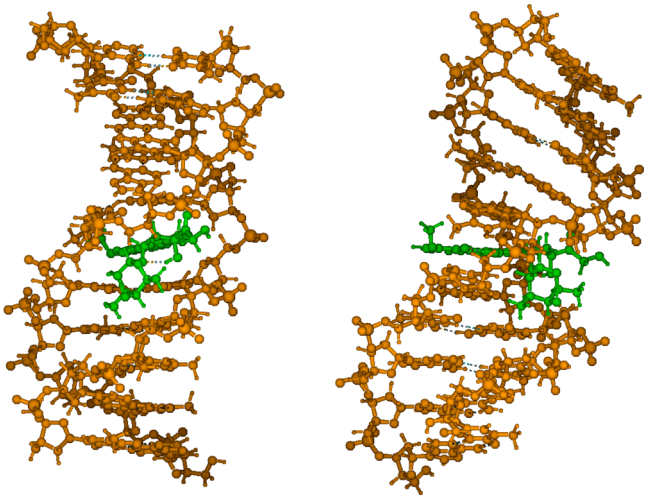

Figure 4. Amber three-dimensional models for the doxorubicin−polyAT system.

three-dimensional models obtained for the intercalation of doxorubicin in the polyAT and polyGC double helices, respectively, are shown. To the best of our knowledge, no crystallographic studies have been reported on interaction complexes between doxorubicin and synthetic polynucleotides of the AT or GC type, and only data relative to the interaction of DX and DNR with hexanucleotide duplexes of mixed sequence exist.[45] For this reason, the structural comparison was performed only with the B conformation of native DNA. Furthermore, we point out that the experimental spectroscopic techniques exploited in this work supply data relative to all possible kinds of mechanisms for interaction between the drug and the two polynucleotides. On the other hand, the MM calculations, within the limits of the approximations both in the calculation method and in the model systems chosen, provide structural information about only the drug−polynucleotide intercalation mechanism. It is finally to be stressed that the

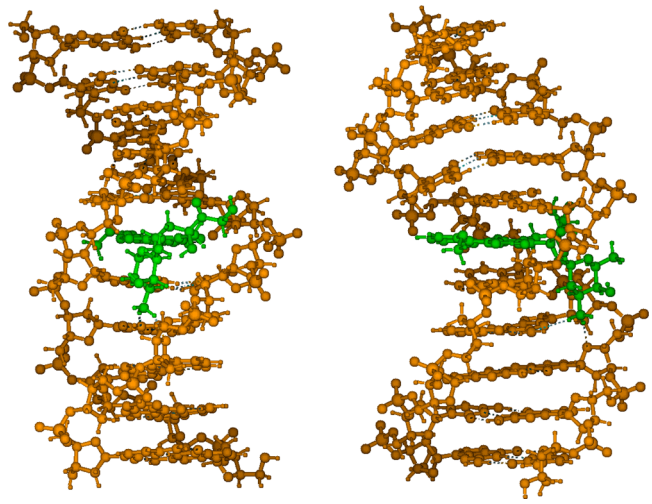

Figure 5. Amber three-dimensional models for the doxorubicin−polyGC system.

crystallographic structures of the doxorubicin−oligonucleotide complexes provide information about bridged water molecules that mediate the drug−oligonucleotide interaction,[45] while in the intercalation complex models chosen, the solvent was not explicitly considered.

The qualitative analysis of the torsional angles of the sugar−phosphate backbone of the doxorubicin−d(ATATATATAT)$_2$ and doxorubicin−d(GCGCGCGCGC)$_2$ complexes (see Figures 4 and 5, respectively) shows that the three complementary residues involved in specific interactions with doxorubicin, i.e., the fourth, fifth, and sixth base pairs in the intercalation pocket, are quite distorted compared to those of B-DNA, while the other residues still keep a B-DNA conformation, in agreement with literature data.[45] For both decanucleotide models, the planar system of rings B−D of doxorubicin is parallel to the plane of the DNA bases in the intercalation pocket, and essentially perpendicular to the double-helix axis. Despite the consistent distortions of the double helix of the two decanucleotides as a consequence of the intercalation, both the pucker angle (C2′-endo) and the glycosidic bond are those of a right-handed double helix of the B type.

The analysis of the average values of the torsional angles obtained shows that larger deviations from the B-DNA conformation have been observed for d(ATATATATAT)$_2$ than for d(GCGCGCGCGC)$_2$. As a consequence of the larger distortions for the d(AT) decanucleotide duplex, the planar aromatic ring system of DX, which spans the whole width of the double helix, protrudes with its D ring into the widened major groove, coming in contact with a highly charged environment. The direct hydrogen bond distances, with no bridging water, are more (i.e., 5 vs 4) in the intercalation complex of doxorubicin with d(GCGCGCGCGC)$_2$ than in that with d(ATATATATAT)$_2$. Such a result, taken alone, would suggest the existence of a higher affinity of the drug for intercalation in the GC-type than in AT-type decanucleotide. Interestingly, this result is in agreement with literature findings concerning the preference of anthracyclines to intercalate GC rather than AT base pairs in mixed sequence oligonucleotides.[45] However, on the basis of the calculated structure for the intercalation complex of polyAT (Figure 4), it is also possible to envisage a water-bridged hydrogen bonding interaction between the daunosamine charged group, which lies in the

dx.doi.org/10.1021/bi401687v | Biochemistry 2014, 53, 2197−2207

minor groove, and the C-2 carbonyl group of the thymine of an adjacent base pair toward which it points, that is not involved in the W-C base pairing.

Fluorescence Studies. The interaction between DX and polyGC does not lead to any band shift in the drug emission spectra, thus meaning that in the presence of polyGC the fluorescence of the bound DX is totally quenched and the observed fluorescence results solely from the nonassociated drug molecule. In fact, for an R value of 8.5, the complete disappearance of the DX fluorescence is observed (Figure S5 of the Supporting Information). This allows $[DX]_f$ to be obtained from the calibration plot (see Materials and Methods and Figure S1 of the Supporting Information). Fluorescence lifetime measurements reveal indeed that upon binding to polyGC the decay is always monoexponential, with a lifetime of 1.00 ns, typical of the monomeric form of DX in water.[46,47] Apart from being a strong indication of the static nature of the quenching process,[48] this means that the F/F_0 ratio (where F is the fluorescence intensity recorded after the addition of any amount of polyGC and F_0 the initial DX fluorescence intensity) is actually the mole fraction of the free doxorubicin. Therefore, it is straightforward to calculate the concentration of the free drug as $[DX]_f = [DX]_a \times F/F_0$. In the case of DX titrated with polyGC, this represents an internal control of the reliability of both the calibration plot and the assumption of the totally quenched DX fluorescence upon interaction with polyGC. In fact, the $[DX]_f$ values calculated in these two ways never differ for more than 1% (see Figure S6 of the Supporting Information).

The fluorescence static quenching of the DX emission upon binding to polyGC (Figure 6) shows the positive deviation

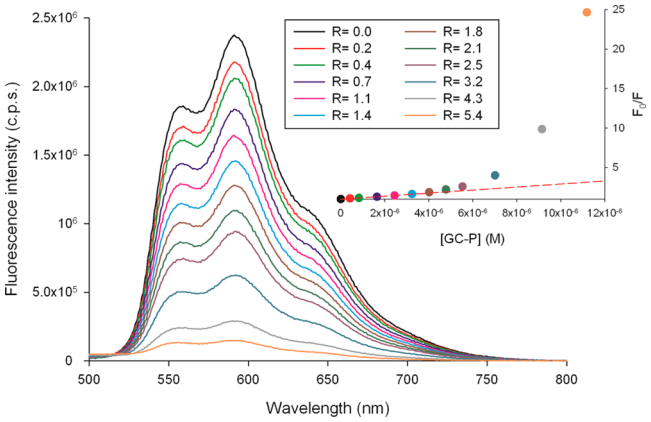

Figure 6. Titration of doxorubicin with polyGC: fluorescence emission spectra (298 K; 1 mM PB, pH 7.4; initial $[DX]_a$ = 2.3 μM; λ_{exct} = 410 nm; slits of 5 and 5 nm; l = 1 cm). The inset shows fluorescence quenching as a function of [GC-P] (the dashed line is the best fit according to the Stern–Volmer equation).

from the Stern–Volmer equation frequently observed when the extent of quenching is large.[48] In such cases, only the linear part of the plot has been fit to the Stern–Volmer equation (see the dashed line in the inset of Figure 6), to obtain information about the order of magnitude of the fluorophore–quencher interaction constant under the different conditions explored.

The data regarding the interactions of DX with polyAT seem more intriguing, because in this case a band red-shift was observed in the emission spectra of the drug. The size of such a shift (8 nm) and the only partial quenching observed (40% at the most, agreeing quite well with literature data[14]) are indications of an incomplete intercalative binding mode, but still with a spatial proximity between the fluorophore and the quencher. Different experiments have been performed on the DX–polyAT system by varying $[DX]_a$. In any case, the observed quenching strictly followed the Stern–Volmer relationship, never showing the superlinear trend shown by polyGC (see the inset of Figure 6). For different values of $[DX]_a$, however, different values of the Stern–Volmer constant (K_{SV}, reported in the legend of Figure 7) were obtained. Such a

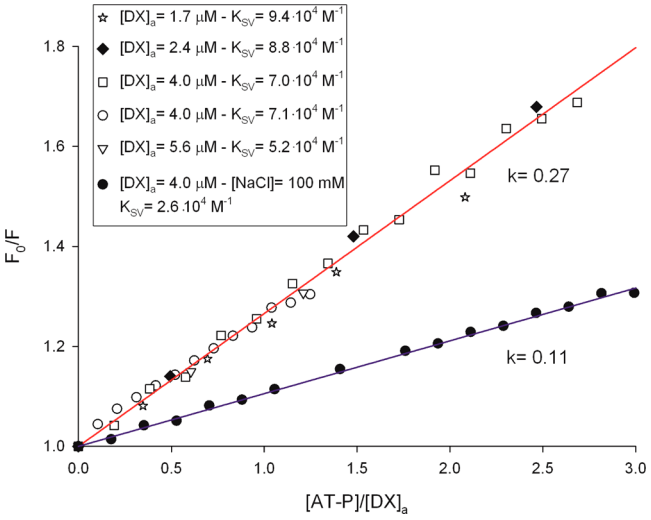

Figure 7. Modified Stern–Volmer plot for the doxorubicin–polyAT system for different values of $[DX]_a$, with and without NaCl (298 K; 1 mM PB, pH 7.4). Lines are the best fits according to the relation $F_0/F = 1 + kR$.

discrepancy disappeared when F_0/F values were plotted against R instead of the quencher concentration ($[AT-P]_a$, in this instance), all the data then lying on the same master curve (Figure 7). In the DX–polyAT interaction, what does matter is the relative concentration of the fluorophore and quencher rather than their absolute concentration. For R values of >3, however, negative deviations from the Stern–Volmer relationship were observed (see the inset of Figure 8), as already observed in the literature[49] for the DX quenching by AMP.

As already described, the interaction between the DX and the polyAT leads to the formation of an association product that is still fluorescent, although with a reduced fluorescence quantum yield and red-shifted compared to the parent DX, with the two forms apparently in equilibrium with each other. To obtain information about this last instance, the decays of the DX fluorescence signals at wavelengths characteristic of the DX emission spectrum, namely, 560, 595, and 640 nm, along a titration with polyAT in PB buffer have been measured (Figure 9). In the presence of polyAT, the decays are always described by the sum of two exponentials, with lifetimes that remain constant along the titration at 1.00 ns (that can easily be ascribed to the free DX[46,47]) and 1.80 ns (relative to the bound DX).[50] What does change is their relative weight (see Figure S7a–c of the Supporting Information) that, when plotted against R, leads to a classical binding isotherm that can be fit to a sigmoidal curve (see the inset of Figure 9), whose inflection point indicates that 50% of DX is bound to approximately 1.5 AT base pairs. This, again, is an indication of an intercalative mode of binding of DX to polyAT, because groove binding

dx.doi.org/10.1021/bi401687v | Biochemistry 2014, 53, 2197–2207

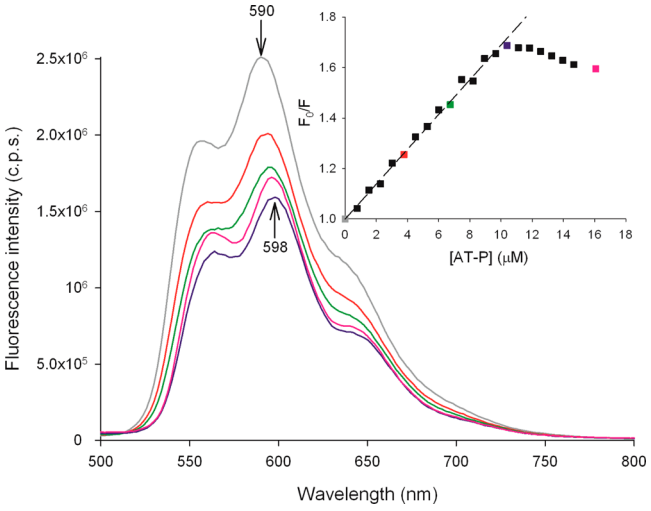

Figure 8. Titration of doxorubicin with polyAT. A selection of fluorescence spectra recorded along the titration is shown (298 K; 1 mM PB, pH 7.4; initial $[DX]_a$ = 4.0 μM; λ_{exct} = 410 nm; slits of 5 and 5 nm; l = 1 cm). The inset shows a Stern–Volmer plot for the whole experiment (color points refer to the spectra in the main graph). The dashed line is the best fit to the Stern–Volmer equation limited to the linear part of the plot, giving a K_{SV} of 7.0 × 10^4 M^{-1}.

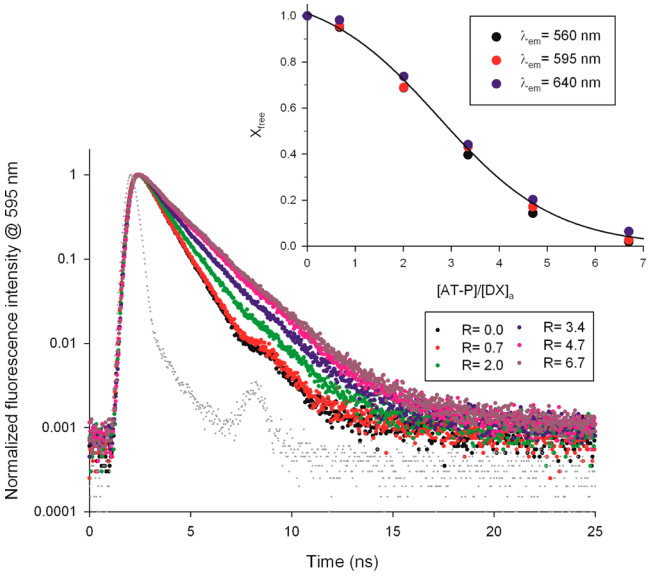

Figure 9. Doxorubicin fluorescence lifetime measurements as a function of R (298 K; 1 mM PB, pH 7.4; initial $[DX]_a$ = 2.4 μM; λ_{exct} = 378 nm; Corning 3391 filter; l = 1 cm). Gray points refer to the IRF acquired at the same wavelength as the decays (595 nm, in this instance), by using the Rose Bengal emission in water.[19] The inset shows the fraction of free doxorubicin deduced from lifetime data acquired at three different wavelengths (see the text for details). The solid line is the global best fit according to a classical binding isotherm.

would have led to higher values of the exclusion parameter(s).[51] It is interesting to note that the blue spectrum in Figure 8 almost corresponds, as an R value, to the inflection point of the sigmoid (inset of Figure 9). Even though after this point the DX lifetimes (free and bound) do not change, the spectra do (compare blue and pink spectra in Figure 8). Again, this is an indication that even when the system shows the negative deviations from the Stern–Volmer relationship, the main characteristics of the bound form of DX are retained (position of the fluorescence peak and lifetime). With respect to the fluorescence lifetimes of DX bound to polyAT, it has to be added that they show the same value of 1.80 ns at the three wavelengths also in the case of polyAT titrated with DX, i.e., in a large excess of binding sites (data not shown).

Because the interaction between DX and polyAT seems to lead to the formation of a single product, an attempt has been made to extract quantitative information about the equilibrium constant ruling the interaction from the fluorescent spectra recorded along a titration of DX with polyAT. By assuming that the fluorescence spectrum of the DX–polyAT system when all the DX is bound to polyAT is that showing the larger red-shift (e.g., the blue spectrum in Figure 8), a linear combination of this spectrum with that of pure doxorubicin allowed the mole fraction of free DX (X_{free}) to be extracted from each intermediate spectrum along a titration (Figure S8 of the Supporting Information), and from these data, the relevant association constant was determined (see Binding Constant Determination).

The interaction between DX and polyAT differs from that with polyGC, as is also evidenced by the fluorescence excitation spectra recorded along a DX titration with polyAT (Figure 10).

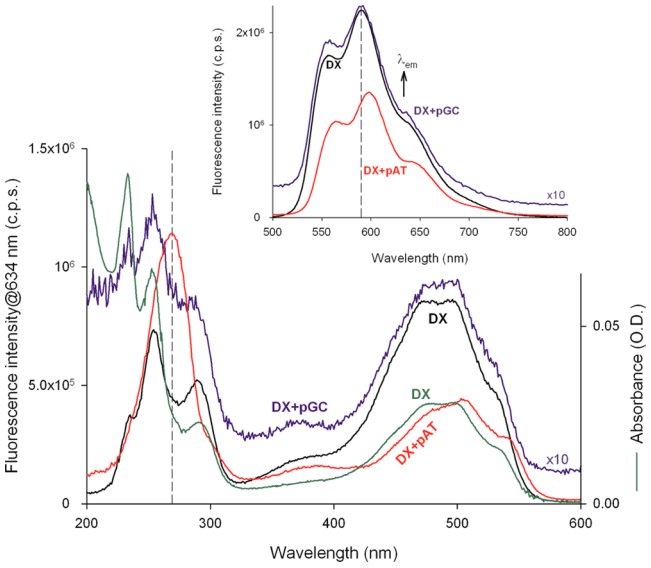

Figure 10. Fluorescence excitation spectra (left-hand axis) of DX with and without added polynucleotides (298 K; 1 mM PB, pH 7.4; $[DX]_a$ = 2.4 μM; R = 4.5; λ_{em} = 634 nm; slits of 5 and 5 nm; BA 590 filter; l = 1 cm) and DX absorption spectrum (green line, right-hand axis). The inset shows the fluorescence emission spectra of the same systems (λ_{exct} = 410 nm; slits of 5 and 5 nm); the arrow indicates the wavelength at which the fluorescence excitation spectra have been acquired while the dashed line the 590 nm position of the DX emission maximum. Both excitation and emission spectra of the DX–polyGC system have been multiplied by a factor of 10.

These data reveal the presence of a strong energy transfer process from polyAT to DX, resulting in a strong band in the excitation spectra centered at 270 nm (see also Figure S9 of the Supporting Information), not present in the results of analogous experiments performed with polyGC, where the quenching of the fluorescence signals is the only detected effect of the interaction. Even the representation of the fluorescent excitation data of the polyGC–DX system according to LePecq[52] does not allow any energy transfer band to be evidenced (data not shown). Analogous situations are often

dx.doi.org/10.1021/bi401687v | Biochemistry 2014, 53, 2197–2207

found in the literature when polyGC is involved in interactions with intercalating agents based on an anthracene core (see, e.g., ref 53). Of interest is the situation shown by the excitation spectra of DX acquired along a titration with ct-DNA. At the beginning (low R values), the prevailing effect is the attenuation of the fluorescence signals that parallels what was observed along a DX titration with polyGC. At high R values, however, a band centered approximately at 270 nm appears (see Figure 11), clearly indicating that the DX intercalates into GC pairs as well as into AT regions.

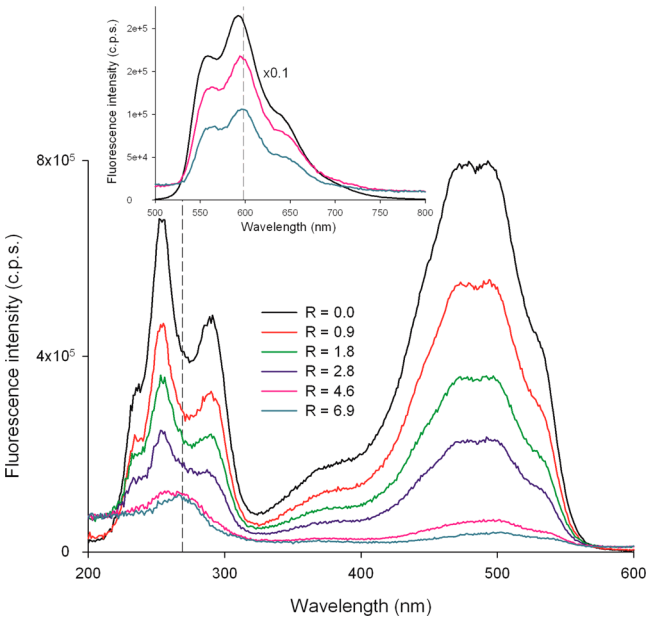

Figure 11. Fluorescence excitation spectra of DX in the presence of increasing amounts of ct-DNA (298 K; 1 mM PB, pH 7.4; $[DX]_a$ = 2.4 μM; λ_{em} = 634 nm; slits of 5 and 5 nm; BA 590 filter; l = 1 cm). The dashed line indicates the 270 nm wavelength. The inset shows a selection of fluorescence emission spectra for the same system (λ_{exct} = 410 nm; slits of 5 and 5 nm; colors as in the main graph; the black curve has been mathematically multiplied by 0.1); the dashed line indicates a wavelength of 598 nm.

Binding Constant Determination. Two different fitting equations were used for the calculation of the binding parameters K_B, the apparent binding constant, and s, the length of the binding site in base pairs. McGhee–von Hippel's equation[54] (eq 1), which requires a constant polynucleotide concentration, was employed when polyGC was titrated with the drug:

$$\frac{r}{[DX]_f} = K_B(1 - sr)\left(\frac{1 - sr}{1 - sr + r}\right)^{s-1} \quad (1)$$

where r is the $[DX]_b/[GC]_{bp}$ ratio, where $[DX]_b$ is the concentration of bound DX and $[GC]_{bp}$ the constant concentration of the polynucleotide in base pairs.

For the titrations of DX with one of the polynucleotides, namely when $[DX]_a$ was kept constant along the titration, Carter's equation[55] (eq 2) was instead used:

$$[DX]_b = \frac{b - \sqrt{b^2 - \frac{2K_B^2[DX]_a[PN\text{-}P]}{s}}}{2K_B} \quad (2)$$

where b is given by

$$b = 1 + K_B[DX]_a + \frac{K_B[PN\text{-}P]}{2s}$$

PolyGC was titrated with DX in 1 mM PB (pH 7.4) in the presence of NaCl at different concentrations, namely, 0, 1, 10, 25, 50, and 100 mM. The initial polyGC concentration was in the range of 25–30 μM in monomer units, and R was varied between 9.1 and 5.5. At higher R values, the fluorescence signal, which is due to free DX, was too low to be measurable. UV–vis and fluorescence spectra of each sample were recorded, and the experimental data were processed making use of eq 1. $[GC]_{bp}$ and $[DX]_a$ were obtained from the UV–vis spectra as indicated in Materials and Methods. $[DX]_b$ was obtained as the difference $[DX]_a - [DX]_f$, where $[DX]_f$ was obtained by interpolation of the calibration curve (Figure S1 of the Supporting Information). Fitting of the plots of $r/[DX]_f$ versus r yielded the values of K_B and s listed in Table 2.

Table 2. Apparent Binding Constants (K_B) and Binding Site Lengths in Base Pairs (s) for the PolyGC–DX System (298 K; 1 mM PB, pH 7.4)

[NaCl] (mM)	K_B ($\times 10^{-6}$ M^{-1})[a]	s[a]
0.0	21.1 ± 0.5	1.8 ± 0.1
1.0	14.6 ± 0.8	1.7 ± 0.1
10.0	6.7 ± 0.3	1.6 ± 0.1
25.0	7.4 ± 0.2	1.8 ± 0.1
50.0	4.2 ± 0.1	2.6 ± 0.1
100.0	5.4 ± 0.2	2.8 ± 0.1

[a] ± fitting error.

The K_B values show a strong dependence on ionic strength, sharply decreasing from a high value in the absence of NaCl to an almost constant lower value when the amount of added salt is increased. This behavior implies an electrostatic contribution to the binding, possibly connected with the positively charged daunosamine fragment accommodated into the minor groove.[56]

The binding constants of DX with polyGC, polyAT, and ct-DNA were obtained from the fluorometric titrations of DX with the three polynucleotides in the absence of NaCl and with 100 mM salt making use of eq 2.

Fitting the plots of $[DX]_b$ versus [PN-P] yielded the values of K_B and s listed in Table 3. $[DX]_f$ was obtained from the calibration curve (Figure S1 of the Supporting Information) in the case of polyGC and ct-DNA. Alternatively, because of the total quenching of fluorescence shown by DX in the presence of polyGC, $[DX]_f$ has been estimated as outlined in Fluorescence Studies.

For polyAT, the formation of a fluorescent association product required a different approach to evaluate the mole fraction of free DX, as outlined in Fluorescence Studies. In the case of polyAT and ct-DNA, the titration of DX was also followed by UV–vis spectroscopy. In these cases, the $[DX]_b$ values were obtained directly from the spectral data by means of the following equation:[9]

$$[DX]_b = \frac{A_s - A_f}{A_b - A_f}[DX]_a \quad (3)$$

where A_s, A_f, and A_b are the absorbance of the drug of each sample, in the absence of the polynucleotide and bound to the complex at a certain wavelength. The value of 480 nm was chosen for the calculations, because only DX absorbs at this wavelength. For polyAT, A_b was obtained from the spectra at R

dx.doi.org/10.1021/bi401687v | Biochemistry 2014, 53, 2197–2207

Table 3. Average Quenching Constants (K_{SV}) and Apparent Binding Parameters (±half-dispersion) for Doxorubicin with Different Polynucleotides (298 K; 1 mM PB, pH 7.4)

polynucleotide	[NaCl] (mM)	K_{SV} (M^{-1})	K_B (M^{-1})	s (bp)
polyAT	0	$(7.5 \pm 2.1) \times 10^4$	$(6.6 \pm 0.6) \times 10^6$	0.9 ± 0.1
	100	$(2.6 \pm 0.8) \times 10^4$	not determined	not determined
polyGC	0	$(8.2 \pm 1.6) \times 10^5$	$(3.3 \pm 1.4) \times 10^6$	1.2 ± 0.8
	100	$(8.8 \pm 0.9) \times 10^4$	$(2.4 \pm 0.3) \times 10^6$	1.8 ± 0.1
ct-DNA	0	$(2.3 \pm 0.8) \times 10^5$	$(2.0 \pm 0.5) \times 10^6$	1.7 ± 0.1
	100	$(4.7 \pm 0.7) \times 10^4$	$(3.67 \pm 0.42) \times 10^{6a}$	0.15 ± 0.05^a

[a]In 50 mM PB, 50 mM NaCl, and 1 mM EDTA (pH 6.2). Data from ref 14.

values above ~4.3, because no change was observed in the spectral region above >350 nm upon further addition of the polynucleotide. For ct-DNA, the A_b at 480 nm was extracted from the spectra at R above 6, when the drug appears to be totally bound to the polymer. In principle, the binding constants from fluorescence and UV−vis data could be different, because fluorescence reflects only intercalative interactions, which lead to quenching, while UV−vis is sensitive to all types of binding. However, no significant difference was observed between the two sets of data, further supporting the conclusion based on the spectral data discussed above that intercalation is essentially the only type of interaction of DX with the three polynucleotides.

One point, however, requires some comment. The K_B values listed in Table 3 for polyGC are considerably lower than the K_B values at the matching NaCl concentrations listed in Table 2.

The discrepancy might arise from the different way by which R is changed in the two series of experiments. This is indeed a critical factor, as evidenced also by the different evolutions of the CD spectra (compare the spectra in Figures 1 and 2).

When polyGC is titrated with DX, the magnitude of the ICD band (Figure 1) attributed to the bound drug increases with R decreasing from 42 [or 160 (data not shown)] to 5.6, to remain unchanged upon further addition of the drug, due to saturation of the intercalation sites. On the other hand, when polyGC is added to DX, at the beginning the drug in large excess would occupy all possible binding sites of the double helix, by intercalation or by other mechanisms. Further addition of polyGC would induce a redistribution of the DX, which would progressively occupy the newly available sites with a preference for intercalation over other weaker interactions. Such a picture of system evolution in the course of the titration is reflected by the CD spectral results (Figure 2): the magnitude of the ICD band attributed to intercalated DX increases in the whole R range explored at the expense of the band at 288 nm of the free drug, while the other bands of DX do not change for R values above ~0.9. It might well be that the deformations to the double helix caused by the large excess of associated drug are, at least in part, intrinsically not reversible. Thus, the two types of titration possibly refer to situations that are intrinsically nonequivalent.

CONCLUSIONS

The interaction of DX with polynucleotides is correctly described as intercalation of the drug aglycone moiety between adjacent nucleotide base pairs, with the amino sugar buried in the B helix minor groove. The data presented in this paper on one hand confirm what is already known about this topic from the literature but on the other add are strong experimental evidence of the kind of interaction between DX and polyAT. The preferential binding of DX to the GC site has been always interpreted as a sort of selection rule, meaning that AT sites were not considered to be as suitable for DX.[14,45] The data here presented point to a completely different situation, with the DX affinity for the two different binding sites practically indistinguishable. The experimental evidence leading to this conclusion will be shortly summarized. From the CD spectra, an ICD band analogous to that shown by the DX−polyGC system is present when the drug is titrated with polyAT (Figure 3). Even the magnitude of such an ICD band is on the same order of magnitude, 10 M^{-1} cm^{-1} (in $\Delta\varepsilon$ unit), as that exhibited by the related DX−polyGC system. The appearance of this ICD signal is joined to the disappearance of the polyAT CD signal at 250 nm and to the strong hypochromism revealed by UV−vis spectroscopy upon the first addition of DX to a polyAT solution (Figure S3 of the Supporting Information). Moreover, in the presence of DX, a large increase in the polyAT melting temperature is observed relative to that of the parent system [ΔT_m values of 33 K at 25 mM NaCl and >60 K in PB buffer (see Table 1)].

From the fluorescence data, the spatial proximity of DX and polyAT is deduced, which results in the formation of an association product characterized by an emission spectrum 8 nm red-shifted with respect to the fluorescence spectrum of DX alone (Figure 8). Titrations of DX solutions with polyAT reveal the presence of only two species in equilibrium, namely, free and bound DX, as determined by both steady-state (Figure S8 of the Supporting Information) and time-resolved (Figure 9) fluorescence. The resulting binding isotherm, fit to Carter's equation (inset of Figure S8 of the Supporting Information), is characterized by small values of the exclusion parameter (s), a further strong indication of the intercalative mode of binding of DX to polyAT (Table 3). A very strong transfer of energy from polyAT to DX is evidenced by the fluorescence excitation spectra (Figure 10 and Figure S9 of the Supporting Information) that support the spatial proximity of the aromatic system of polyAT nucleobases and the DX fluorophore. This band is probably present also in the DX−polyGC system, but because of the optimal overlapping of the aromatic system of DX with the GC pocket, which results in a 100% quenching of DX in the presence of polyGC, it is not experimentally elucidated. MM calculations offer the key to interpreting the different fluorescent properties shown by DX when it is bound to a GC or AT binding site. In the last case, in fact, ring D of DX protrudes into a widened major groove of the polyAT molecule (Figure 4). This would explain both the only partial quenching of the DX fluorescence and the 8 nm shift in the emission spectrum of DX bound to polyAT, due to the exposure of the fluorophore (or, at least, of part of it) to a very polar environment.

The strong affinity of DX for GC and AT binding sites is also confirmed by the fluorescence excitation spectra recorded for

dx.doi.org/10.1021/bi401687v | Biochemistry 2014, 53, 2197−2207

the DX−ct-DNA system. At high R values, i.e., when most of the fluorescence of the free DX has been quenched, both emission and excitation spectra of DX reveal the same features observed in the presence of polyAT, i.e., 8 nm red shift in the emission spectrum and the energy band transfer centered at 270 nm (Figure 11).

■ ASSOCIATED CONTENT

Supporting Information

Figures S1−S9. This material is available free of charge via the Internet at http://pubs.acs.org.

■ AUTHOR INFORMATION

Corresponding Author

*E-mail: mauro.giustini@uniroma1.it. Telephone: +39-06-49913336. Fax: +39-06-490324.

Funding

The financial support of the Universities of Palermo and Rome "La Sapienza" is gratefully acknowledged. M.G. thanks C.S.G.I (O.U. of Bari) for partial financial support.

Notes

The authors declare no competing financial interest.

■ ACKNOWLEDGMENTS

This work is dedicated to our dearest friend Marcello, who planned most of the experiments reported here.

■ ABBREVIATIONS

DX, doxorubicin; DNR, daunorubicin; polyAT, poly(dA-dT)·poly(dA-dT); polyGC, poly(dG-dC)·poly(dG-dC); ct-DNA, calf thymus DNA; PB, phosphate buffer.

■ REFERENCES

(1) Lown, J. W. (1996) Discovery and development of anthracycline antitumour antibiotics. *Chem. Soc. Rev. 22*, 165−176.

(2) Saenger, W. (1984) *Principles of nucleic acids structure*, Springer-Verlag, New York.

(3) Miroshnychenko, K. V., and Shestopalova, A. V. (2010) The effect of drug-DNA interactions on the intercalation site formation. *Int. J. Quantum Chem. 110*, 161−176.

(4) Graves, D. E., and Velea, L. M. (2000) Intercalative binding of small molecules to nucleic acids. *Curr. Org. Chem. 4*, 915−929.

(5) Neidle, S., and Abraham, Z. (1984) Structural and sequence-dependent aspects of drug intercalation into nucleic acids. *Crit. Rev. Biochem. Mol. Biol. 17*, 73−121.

(6) Chaires, J. B. (1983) Equilibrium studies on the interaction of daunomycin with deoxypolynucleotides. *Biochemistry 22*, 4204−4211.

(7) Garbesi, A., Bonazzi, S., Zanella, S., Capobianco, M. L., Giannini, G., and Arcamone, F. (1997) Synthesis and binding properties of conjugates between oligodeoxynucleotides and daunorubicin derivatives. *Nucleic Acids Res. 25*, 2121−2128.

(8) Chaires, J. B., Dattagupta, N., and Crothers, D. M. (1982) Studies on interaction of anthracycline antibiotics and deoxyribonucleic acids: Equilibrium binding studies on interaction of daunomycin with deoxyribonucleic acid. *Biochemistry 21*, 3933−3940.

(9) Xodo, L. E., Manzini, G., Ruggiero, J., and Quadrifoglio, F. (1988) On the interaction of daunomycin with synthetic alternating DNAs: Sequence specificity and polyelectrolyte effects on the intercalation equilibrium. *Biopolymers 27*, 1839−1857.

(10) Hajian, R., Shams, N., and Mohagheghian, M. (2009) Study on the interaction between doxorubicin and deoxyribonucleic acid with the use of methylene blue as a probe. *J. Braz. Chem. Soc. 20*, 1399−1405.

(11) Patel, K. K., Plummer, E. A., Darwish, M., Rodger, A., and Hannon, M. J. (2002) Aryl substituted ruthenium bis-terpyridine complexes: Intercalation and groove binding with DNA. *J. Inorg. Biochem. 91*, 220−229.

(12) Spillane, C. B., Smith, J. A., Morgan, J. L., and Keene, F. R. (2007) DNA affinity binding studies using a fluorescent dye displacement technique: The dicotomy of the binding site. *JBIC, J. Biol. Inorg. Chem. 12*, 819−824.

(13) Ghosh, A., Das, P., Gill, M. R., Kar, P., Walker, M. G., Thomas, J. A., and Das, A. (2011) Photoactive Ru^{II}-polypyridyl complexes that display sequence selectivity and high-affinity binding to duplex DNA through groove binding. *Chem.—Eur. J. 17*, 2089−2098.

(14) DuVernay, V. H., Jr., Pachter, J. A., and Crooke, S. T. (1979) Deoxyribonucleic acid binding studies on several new anthracycline antitumor antibiotics. Sequence preference and structure-activity relationships of marcellomycin and its analogues as compared to adriamycin. *Biochemistry 18*, 4024−4030.

(15) Rabbani, A., Finn, R. M., and Ausió, J. (2005) The anthracycline antibiotics: Antitumor drugs that alter chromatin structure. *BioEssays 27*, 50−56.

(16) Cramer, C. J. (2004) *Essentials of computational chemistry*, 2nd ed., Chapter 2, pp 17−68, Wiley, New York.

(17) Airoldi, M., Boicelli, C. A., Gennaro, G., Giomini, M., Giuliani, A. M., and Giustini, M. (2000) A spectroscopic study of poly(dA-dT)·poly(dA-dT) in microemulsions. *Phys. Chem. Chem. Phys. 2*, 4636−4641.

(18) Fiallo, M. M. L., Tayeb, H., Suarato, A., and Garnier-Suillerot, A. (1998) Circular dichroism studies on anthracycline antitumor compounds. Relationship between the molecular structure and the spectroscopic data. *J. Pharm. Sci. 87*, 967−975.

(19) Szabelski, M., Luchowski, R., Gryczynski, Z., Kapusta, P., Ortmann, U., and Gryczynski, I. (2009) Evaluation of instrument response functions for lifetime imaging detectors using quenched Rose Bengal solutions. *Chem. Phys. Lett. 471*, 153−159.

(20) Gennis, R. B., and Cantor, C. R. (1972) Optical studies of a conformational change in DNA before melting. *J. Mol. Biol. 65*, 381−399.

(21) Raguet, J. N., and Brahms, J. (1973) Preliminary investigation of poly(dA-dT) conformation and of its interaction with DNA polymerase. *Biochimie 55*, 111−117.

(22) Ibrahim, M. S. (2001) Voltammetric studies of the interaction of nogalamycin antitumor drug with DNA. *Anal. Chim. Acta 443*, 63−72.

(23) Janssen, M. J. H., Crommelin, D. J. A., Storm, G., and Hulshoff, H. (1985) Doxorubicin decomposition on storage. Effect of pH, type of buffer and liposome encapsulation. *Int. J. Pharm. (Amsterdam, Neth.) 23*, 1−11.

(24) Beijnen, J. H., van der Houwen, O. A. G. J., and Underberg, W. J. M. (1986) Aspects of the degradation kinetics of doxorubicin in aqueous solution. *Int. J. Pharm. (Amsterdam, Neth.) 32*, 123−131.

(25) Beijnen, J. H., Potman, R. P., van Ooijen, R. D., Driebergen, R. J., Voskuilen, M. C. H., Renema, J., and Underberg, W. J. M. (1987) Structure elucidation and characterization of daunorubicin degradation products. *Int. J. Pharm. (Amsterdam, Neth.) 34*, 247−257.

(26) Bouma, J., Beijnen, J. H., Bult, A., and Underberg, W. J. M. (1986) Anthracycline antitumour agents. *Pharm. Weekbl., Sci. Ed. 8*, 109−133.

(27) Ponder, J. W. (2001) *TINKER: Software Tools for Molecular Design*, version 3.9, Washington University School of Medicine, St. Louis.

(28) Ren, P., and Ponder, J. W. (2003) Polarizable atomic multipole water model for molecular mechanics simulation. *J. Phys. Chem. B 107*, 5933−5947.

(29) Ren, P., and Ponder, J. W. (2002) Consistent treatment of inter- and intra-molecular polarization in molecular mechanics calculations. *J. Comput. Chem. 23*, 1497−1506 and references cited therein.

(30) Wang, J., Cieplak, P., and Kollman, P. A. (2000) How well does a restrained electrostatic potential (RESP) model perform in calculating conformational energies of organic and biological molecules? *J. Comput. Chem. 21*, 1049−1074.

(31) Spinello, A., Terenzi, A., and Barone, G. (2013) Metal complex-DNA binding: Insights from molecular dynamics and DFT/MM calculations. *J. Inorg. Biochem. 124*, 63−69.
(32) Cornell, W. D., Cieplak, P., Bayly, C. I., Gould, I. R., Merz, K. M., Jr., Ferguson, D. M., Spellmeyer, D. C., Fox, T., Caldwell, J. W., and Kollman, P. A. (1995) A second generation force field for the simulation of proteins, nucleic acids and organic molecules. *J. Am. Chem. Soc. 117*, 5179−5197.
(33) Frisch, M. J., et al. (2004) *GAUSSIAN 03*, revision D01, Gaussian, Inc., Wallingford, CT.
(34) Barone, G., Fonseca Guerra, C., Gambino, N., Silvestri, A., Lauria, A., Almerico, A. M., and Bickelhaupt, F. M. (2008) Intercalation of daunomycin into stacked DNA base pairs. DFT study of an anticancer drug. *J. Biomol. Struct. Dyn. 26*, 115−130 and references cited therein.
(35) Kumar, C. V., and Asuncion, E. H. (1993) DNA binding studies and site selective fluorescence sensitization of an anthryl probe. *J. Am. Chem. Soc. 115*, 8547−8553.
(36) Allenmark, S. (2003) Induced circular dichroism by chiral molecular interaction. *Chirality 15*, 409−422.
(37) Ismail, M. A., Sanders, K. J., Fennell, G. C., Latham, H. C., Wormell, P., and Rodger, A. (1998) Spectroscopic studies of 9-hydroxyellipticine binding to DNA. *Biopolymers 46*, 127−143.
(38) Suh, D., and Chaires, J. B. (1995) Criteria for the mode of binding of DNA binding agents. *Bioorg. Med. Chem. 3*, 723−728.
(39) Nair, R. B., Teng, E. S., Kirkland, S. L., and Murphy, C. J. (1998) Synthesis and DNA-binding properties of $[Ru(NH_3)_4dppz]^{2+}$. *Inorg. Chem. 37*, 139−141.
(40) Berova, N., Nakanishi, K., and Woody, R. W., Eds. (2000) *Circular dichroism: Principles and applications*, 2nd ed., Chapter 26, pp 741−768, Wiley-VCH, New York.
(41) Cui, F., Huo, R., Hui, G., Lv, X., Jin, J., Zhang, G., and Xing, W. (2011) Study on the interaction between aglycon of daunorubicin and calf thymus DNA by spectroscopy. *J. Mol. Struct. 1001*, 104−110.
(42) Satynarayana, S., Dabrowiak, J. C., and Chaires, J. B. (1993) Tris(phenanthroline)ruthenium(II) enantiomer interactions with DNA: Mode and specificity of binding. *Biochemistry 32*, 2573−2584.
(43) Cusumano, M., Di Pietro, M. L., Giannetto, A., and Vainiglia, P. A. (2005) The intercalation to DNA of bipyridyl complexes of platinum(II) with thioureas. *J. Inorg. Biochem. 99*, 560−565.
(44) Bjorndal, M. T., and Fygenson, D. K. (2002) DNA melting in the presence of fluorescent intercalating oxazole yellow dyes measured with a gel-based assay. *Biopolymers 65*, 40−44.
(45) Frederick, C. A., Williams, L. D., Ughetto, G., van der Marel, G. A., van Boom, J. H., Rich, A., and Wang, A. H.-J. (1990) Structural comparison of anticancer drug-DNA complexes. Adriamycin and daunomycin. *Biochemistry 29*, 2538−2549.
(46) Anand, R., Ottani, S., Manoli, F., Manet, I., and Monti, S. (2012) A close-up on doxorubicin binding to γ-cyclodextrin: An elucidating spectroscopic, photophysical and conformational study. *RSC Adv. 2*, 2346−2357.
(47) Changenet-Barret, P., Gustavsson, T., Markovitsi, D., Manet, I., and Monti, S. (2013) Unravelling molecular mechanism in the fluorescence spectra of doxorubicin in aqueous solution by femtosecond fluorescence spectroscopy. *Phys. Chem. Chem. Phys. 15*, 2937−2944.
(48) Lakowicz, J. R. (2006) *Principles of fluorescence spectroscopy*, 3rd ed., Chapter 8, pp 282−284, Springer Science+Business Media, New York.
(49) Htun, T. (2004) A negative deviation from Stern-Volmer equation in fluorescence quenching. *J. Fluoresc. 14*, 217−222.
(50) Chen, H.-T., Wu, C.-T., Chung, C.-Y., Hwu, Y., Cheng, S.-H., Mou, C.-Y., and Lo, L.-W. (2012) Probing the dynamics of doxorubicin-DNA intercalation during the initial activation of apoptosis by fluorescence lifetime imaging microscopy (FLIM). *PLoS One 7*, e44947.
(51) Viola, G., Ihmels, H., Kraußer, H., Vedaldi, D., and Dell'Acqua, F. (2004) DNA-binding and DNA-photocleavaging of 12a,14a,diazoniapentaphene. *ARKIVOC (Gainesville, FL, U.S.)*, 219−230.
(52) Le Pecq, J.-B., and Paoletti, C. (1967) A fluorescent complex between ethidium bromide and nucleic acids. Physical-chemical characterization. *J. Mol. Biol. 27*, 87−106.
(53) Kumar, C. V., Punzalan, E. H. A., and Tan, W. B. (2000) Adenine-thymine base pair recognition by an antrhtyl probe from the DNA minor groove. *Tetrahedron 56*, 7027−7040.
(54) McGhee, J. D., and von Hippel, P. H. (1974) Theoretical aspects of DNA-protein interactions: Cooperative and non-cooperative binding of large ligands to a one-dimensional homogeneous lattice. *J. Mol. Biol. 86*, 469−489.
(55) Carter, M. T., Rodriguez, M., and Bard, A. J. (1989) Voltammetric studies of the interaction of metal chelates with DNA. 2. Tris-chelated complexes of cobalt(III) and iron(II) with 1,10-phenantroline and 2,2′-bipyridine. *J. Am. Chem. Soc. 111*, 8901−8911.
(56) Chaires, J. B., Satyanarayana, S., Suh, D., Fokt, I., Przewloka, T., and Priebe, W. (1996) Parsing the free energy of anthracycline antibiotic binding to DNA. *Biochemistry 35*, 2047−2053.